

The potential leaching and mobilization of trace elements from FGD-gypsum of a coal-fired power plant under water re-circulation conditions

Citation for published version:

Cordoba-Sola, P, Castro, I, Maroto-Valer, MM & Querol, X 2015, 'The potential leaching and mobilization of trace elements from FGD-gypsum of a coal-fired power plant under water re-circulation conditions', *Journal of Environmental Sciences*, vol. 32, pp. 72-80. <https://doi.org/10.1016/j.jes.2014.11.009>

Digital Object Identifier (DOI):

[10.1016/j.jes.2014.11.009](https://doi.org/10.1016/j.jes.2014.11.009)

Link:

[Link to publication record in Heriot-Watt Research Portal](#)

Document Version:

Early version, also known as pre-print

Published In:

Journal of Environmental Sciences

Publisher Rights Statement:

© 2015 The Research Center for Eco-Environmental Sciences, Chinese Academy of Sciences. Published by Elsevier B.V.

General rights

Copyright for the publications made accessible via Heriot-Watt Research Portal is retained by the author(s) and / or other copyright owners and it is a condition of accessing these publications that users recognise and abide by the legal requirements associated with these rights.

Take down policy

Heriot-Watt University has made every reasonable effort to ensure that the content in Heriot-Watt Research Portal complies with UK legislation. If you believe that the public display of this file breaches copyright please contact open.access@hw.ac.uk providing details, and we will remove access to the work immediately and investigate your claim.

1 THE POTENTIAL LEACHING AND MOBILISATION OF TRACE ELEMENTS FROM FGD-
2 GYPSUM OF A COAL-FIRED POWER PLANT UNDER WATER RE-CIRCULATION
3 CONDITIONS

4
5 Patricia Córdoba^{1*}, Iria Castro², Mercedes Maroto-Valer¹, Xavier Querol²

6
7 ¹Centre for Innovation on Carbon Capture and Storage (CICCS), Institute of Mechanical,
8 Process and Energy Engineering (IMPEE), Heriot-Watt University, EH14 4AS, United Kingdom.

9 ²Institute of Environmental Assessment and Water Research (IDÆA-CSIC), Jordi Girona 18-26,
10 Barcelona, Spain.

11 *Corresponding author e-mail: pc247@hw.ac.uk

ABSTRACT

Experimental and geochemical modelling studies were carried out to identify mineral and solid phases containing major, minor, and trace elements and the mechanism of the retention of these elements in FGD-gypsum samples from a coal-fired power plant under filtered water recirculation to the scrubber and forced oxidation conditions. The role of the pH and related environmental factors on the mobility of Li, Ni, Zn, As, Se, Mo, and U from FGD-gypsums for a comprehensive assessment of element leaching behaviour were also carried out. Results show that the extraction rate of the studied elements generally increases with decreasing the pH value of the FGD-gypsum leachates. The increase of the mobility of elements such as U, Se, and As in the FGD-gypsum entails the modification of their aqueous speciation in the leachates; UO_2SO_4 , H_2Se , and HAsO_2 are the aqueous complexes with the highest activities under acidic conditions. The speciation of Zn, Li, and Ni is not affected in spite of pH changes; these elements occur as free cations and associated to SO_4^{2-} in the FGD-gypsum leachates. The mobility of Cu and Mo decreases by decreasing the pH of the FGD-gypsum leachates, which might be associated to the precipitation of CuSe_2 and MoSe_2 , respectively. TOF mass spectrometry of the solid phase combined with geochemical modelling of the aqueous phase has proved useful in understanding the mobility and geochemical behaviour of elements and their partitioning into FGD-gypsum samples.

Keywords: geochemical modelling studies; trace elements; leaching; landfills, FGD-gypsum; ToF mass spectrometry

1. INTRODUCTION

Water streams involved in Flue Gas Desulphurisation (FGD) systems from coal-fired power plants may act as retention sinks for some trace pollutants as a result of partial or total dissolution processes (Córdoba et al., 2011; 2013), the efficiency of which largely depends on chemical properties such as the pH and temperature of the solvent and/or the solubility constant of a specific element, among other parameters. Indeed, in FGD systems under operational conditions of water re-circulation into the scrubber, inorganic trace pollutants initially in sub-saturation in FGD waters may reach equilibrium and a subsequent saturation in the water stream after a number of water re-circulations in the scrubber (Córdoba et al., 2011). This process may increase the concentration of trace pollutants in re-circulated waters and give rise to environmental implications such as the emission of elements by entraining particles and droplets of gypsum slurry in the outgoing gaseous stream of the FGD (OUT-FGD) (Córdoba et al., 2011), and/or technical problems, especially if the re-circulation of the water streams is interrupted and/or a water treatment is necessary for hypothetical and eventual discharges to the environment. Other elements retained in high proportions by gypsum sludge and/or FGD-gypsum do not pose this problem because they are extracted from the system by the gypsum by-product.

Although FGD-gypsum reduces the consumption of energy and natural resources, there is a significant concern about the potential release of trace elements in specific applications scenarios. Sanchez et al (2008) found that B, Cd, Mo, Se, and Tl may be released from FGD-gypsum at levels exceeding either a maximum contaminant level (MCL) or Drinking Water Equivalent Level (DWEL) under some conditions. Other authors (Álvarez-Ayuso et al., 2006; 2007; 2008; Font et al., 2008; Córdoba et al., 2013) have reported that elements such as F plays a crucial role in the leaching potential of the FGD gypsum end-product as a consequence of the precipitation of F solid species on FGD-gypsum surface.

Investigations on the effect of external factors on the release of elements such as As, Se and Hg from FGD-gypsum have shown that metal release under natural conditions (pH~7) is not an environmental concern (Kairies et al., 2006; Kost et al., 2005). The high alkalinity of the FGD-

gypsum and the presence of As and Se in sparingly soluble calcium complexes (CaSeO_3 and $\text{Ca}_3\text{As}_2\text{O}_8$) results in low mobilities of the trace metals (Díaz-Somoano et al., 2004; Gou et al., 2004; Jadhav and Fan, 2001; Ghosh-Dastidar et al., 1996). However, metal mobility can be significant at low pH conditions for elements such as Ni, Cu, Li, Mo, Zn, and U. Since metal partitioning and speciation in any solid define their toxicity and mobility, their determination is important in order to understand the environmental consequences of the reuse of FGD-gypsum.

The overall objective of the study is to i) identify solid phases containing major, minor, and trace elements and the mechanism of the retention of the elements in FGD-gypsum; and to ii) evaluate more fully the role of pH and related environmental factors on the mobility of Li, Ni, Zn, As, Se, Mo, and U from FGD-gypsums, as a basis for comprehensive assessment of element leaching behaviour under a range of environmental conditions. This paper presents results obtained from a series of leaching tests of four FGD-gypsum samples from a coal-fired power plant at which the enrichment of inorganic trace pollutants in the re-circulation FGD water has been demonstrated (Cordoba et al., 2012a).

2. MATERIALS AND METHODS

2.1. The FGD system

The FGD system at this power plant involves a number of water streams categorised as FGD water streams: limestone and gypsum slurries and filtered water. A fraction of processed water is treated before it is used to reduce the high content of salts. The resulting water (treated water) is employed for limestone slurry preparation and is then considered as an FGD water stream. An additional fraction of water (added water) is injected into the scrubber to offset the water loss in the gypsum and in the emitted gas. Filtered water is used for limestone slurry preparation, and the remaining fraction is directly recirculated into the scrubber. The mixture of slurry waters constitutes the main water input into the scrubber. The water output of the FGD systems is constituted by i) the aqueous phase of gypsum slurry, ii) the loss of crystallization water from gypsum, and iii) the water evaporation due to the contact with the emitted OUT-FGD gas in the scrubber. These inputs and outputs of water offset the water balance through the

FGD system at the power plant. Detailed descriptions of the operation of the FGD system at this power plant and the water streams are provided by Córdoba et al (2012a).

The four FGD-gypsum samples called FGD-G1, 2, 3, and 4 were collected from this power plant under the filtered water recirculation to the scrubber and forced oxidation conditions.

2.2. Identification of mineral and solid phases on FGD-gypsums

The identification of minor solid phases of trace elements was carried out in addition to X-Ray powder Diffraction (XRD), by Time-of-Flight Secondary Ion Mass Spectrometry (ToF-SIMS) analysis because of their low concentration in the FGD-gypsum. ToF-SIMS is a method of mass spectrometry in which the FGD-gypsum sample is ionised and accelerated by an electric field of a given strength. Since the velocity of the ion depends on the mass-to-charge ratio, the ions acquire the same kinetic energy of other ions with the same charge. The time spent by ions reaching the detector and the experimental parameters allow us to identify the ion mass with great accuracy. Thus, the identification of molecules and ionic clusters such as silicates, sulphates, hydroxides, nitrates, and borates that precipitated on FGD-gypsums may be detected even at low concentrations.

The ToF-SIMS analyses were performed using a ToF-SIMS IV (ION-ToF, Munster, Germany) operated at a pressure of 5×10^{-9} mbar. Samples were bombarded with a pulsed Bismuth liquid metal ion source (Bi_3^{++}), at energy of 25 keV. The gun was operated with a 20 ns pulse width, 0.3 pA pulsed ion current for a dosage lower than 5×10^{11} ions/cm², well below the threshold level of 1×10^{13} ions/cm² generally accepted for static SIMS conditions. Secondary ions were detected with a reflector time-of-flight analyzer, a multichannel plate (MCPs), and a time-to-digital converter (TDC). Measurements were performed with a typical acquisition time of 6s, at a TDC time resolution of 200 ps and 100us cycle time. Charge neutralization was achieved with a low energy (20eV) electron flood gun. Secondary ion spectra were acquired from a randomly rastered surface areas of $50\mu\text{m} \times 50\mu\text{m}$ within the sample's surface. Secondary ions were extracted with 2 kV voltages and are post accelerated to 10 keV kinetic energy just before

hitting the detector. Mass spectral acquisition was performed within the ION-TOF Ion Spec software (version 4.1). Each spectrum was normalised to the total intensity.

2.3. Leaching experiments

Leaching experiments following the standard EN12457-4 according to the Council decision 2003/33/EC were applied to FGD-gypsums in order to define the environmental characteristics concerning the leachability of trace pollutants of these by-products in view of their future disposal in landfills. This consists of a single batch leaching test using Milli-Q (MQ) water as leachant agent at an L/S (liquid to solid) ratio of 10 L/kg and 24h of agitation time in an orbital shaker.

In this study, leaching tests of FGD-gypsum samples were performed at initial pH values of 2.0, 4.0, and at the natural pH of the FGD-gypsum leachates (pH~7); 10/1, 20/1, and 50/1 L/S ratios, and 24, 48, and 168h of agitation time in orbital shaker. The pH values were adjusted to the desired level with diluted H₂SO₄. Three replicates per FGD-gypsum sample and blanks were all prepared in a similar manner.

After leaching tests, the leachates were filtered through 0.45µm filters and divided into two aliquots in High Density Polyethylene (HDPE) bottles. Leachates were then analysed by Inductively-Coupled Plasma Atomic-Emission Spectrometry (ICP-AES) for major and minor elements using the Iris Advantage Radial ER/S device from Thermo Jarrell-Ash. A previous semi-quantitative analysis was carried out to identify the range of element concentrations as well as the matrix and the possible spectral interferences. The calibration was carried out by means of the international certified standard (1000 and 10.000 ppm). Most of the trace elements were analysed by Inductively-Coupled Plasma Mass Spectrometry (ICP-MS) using the X-SERIES II device from Thermo Fisher SCIENTIFIC. The quantitative analysis was carried out using an extern standard with similar matrix of the samples, which covered concentrations range expected forming the calibration lines. The intern correction was carried out by means of an intern standard (In 10 ppb).

The leaching test of FGD-gypsum samples was conducted following the standard EN12457 to (1) obtain the maximum leaching that could be expected from FGD-gypsum in view its disposal in landfills; and (2) according to the particle size of the FGD-gypsum. The standard EN 12457-4 establishes this leaching test for granular waste materials and sludges with particle size below 10 mm (without or with size reduction).

2.4. Geochemical modelling

Simulation tools are usable in a wide range of fields of study from energetic systems and chemical processing of crude oil up to pharmaceutical and food processing industry. These tools facilitate simulation, integration, and optimisation of processes (Andrea Tabasová et al., 2012).

The PHREEQC code (version 2.0) and the coupled thermodynamic database Lawrence Livermore National Laboratory (LLNL) (Parkhurst and Appelo, 1999) were used to calculate the speciation of elements in the leachates from FGD-gypsum samples. The degree of undersaturation or oversaturation of a FGD-gypsum leachate with respect to a particular mineral or solid phase was determined in terms of saturation index (SI), calculated using Eq. (1):

$$SI = \log (IAP/K_{sp}) \quad (1)$$

where IAP is the ion activity product and K_{sp} is the solubility constant for a particular mineral (Drever et al., 1997).

3. RESULTS AND DISCUSSION

3.1. Identification of elements and molecules in FGD-gypsums

Major solid phases ($\text{CaSO}_4 \cdot 2\text{H}_2\text{O}$ and CaCO_3) were identified in the FGD-gypsums by XRD. Mass spectrometry analysis (Table 1) by TOF-SIMS detected Al, Si, Fe, Ca, Mg, Mn, Cl, F, Li, Se, Na, As, and Zn; molecules of CaOH , and Ca_2O_2 ; ionic groups such as SO_3 , SO_4 , and HSO_4 ; monatomic ions of O, and polyatomic such as OH in FGD-gypsums. Molecules of SiO_2 and SO_2 ; cluster ions of SiO_3 , HSiO_3^- , and Se_2O_3 were also identified in FGD-gypsums (Table 1).

Comparison of the intensity signal of major and trace elements among the FGD-gypsum samples reveals a major occurrence of solid phases containing elements such as Al, K, Ca, Fe, and Mn in the FGD-G3. Solid phases containing trace elements such as As, Se, and Zn show a higher intensity in the FGD-G2. The intensity signal of SiO_2 and SO_4 , structural components of major solid phases, is also higher in the FGD-G2. This suggests a major association of SiO_2 and SO_4 with trace elements in the FGD-G2 than in the remaining FGD-gypsums. Indeed, the Ca/ SO_4 intensity ratio is higher in the FGD-G3 and G4 than in FGD-G1 and G2, which indicates that Ca may also precipitate with molecules and/or cluster ions other than SO_4 in the FGD-G3 and G4.

3.2. Occurrence of solid phases: Thermodynamic modelling

Of the solid phases included in the LLNL database (Parkhurst and Appelo, 1999), the geochemical modelling predicts saturation of the aqueous phases in $\text{KAl}_3(\text{OH})_6(\text{SO}_4)_2$, AlO_2H , AlHO_2 , $\text{Al}(\text{OH})_3$, $\text{Al}_2\text{Si}_2\text{O}_5(\text{OH})_4$, and $\text{KAl}_3\text{Si}_3\text{O}_{10}(\text{OH})_2$ in all FGD-gypsum samples (Table 2). This is in agreement with the detection of Al, K, Si cluster ions, and OH in the FGD-gypsums by ToF-SIMS analyses. Aluminium, however, can also occur as $\text{Ca}_2\text{FeAl}_2\text{Si}_3\text{O}_{12}\text{OH}$, $\text{FeCa}_2\text{Al}_2(\text{OH})(\text{SiO}_4)_3$, $\text{CaAl}_2\text{Si}_2\text{O}_7(\text{OH})_2 \cdot \text{H}_2\text{O}$, $\text{CaAl}_4\text{Si}_2\text{O}_{10}(\text{OH})_2$, and/or $\text{NaAl}_3\text{Si}_3\text{O}_{10}(\text{OH})_2$ in the FGD-G3. This could be due to the presence of high levels of aluminosilicate phases (mainly clay minerals). Indeed, an earlier work on the partitioning in the FGD system from this power plant (Cordoba et al., 2012a) demonstrated that Al and Si are supplied by the highly insoluble aluminosilicate fraction of limestone (93% Ca carbonate) and are retained as impurities in the FGD-gypsum sludge. The association of Ca with aluminosilicate phases indicates that Ca can also precipitate in solid phases containing elements and cluster ions other than SO_4^{2-} in the FGD-G3, as it is revealed by the ToF-SIMS analysis.

In addition to the association of Fe with Ca and aluminosilicate phases, this element can also occur as CuFe_2O_4 , ZnFe_2O_4 , FeOOH , Fe_2O_3 , and Fe_3O_4 in the FGD-gypsums. These solid and mineral phases are predicted in saturation in all the FGD-gypsum samples.

Zinc as ZnFe_2O_4 is predicted in saturation in the FGD-gypsums, which is in agreement with the detection of Zn and Fe by ToF-SIMS analysis. Therefore, it could be stated that ZnFe_2O_4 is the most probable specie of Zn in the FGD-gypsum samples.

Although U and Ni are not detected by ToF-SIMS, these elements are detected by ICP-MS analysis in the FGD-gypsum leachates (Table 3). Uranium as $(\text{UO}_2)_2\text{SiO}_4 \cdot 2\text{H}_2\text{O}$ is predicted in saturation in the FGD-G2 and G3 samples.

Solid phases containing Se, Li, As, and Mo are predicted in subsaturation ($\text{SI} < 0$) in the FGD-gypsum samples. However, Se_2O_3 , Li, As, and Mo are identified in all FGD-gypsums by ToF-SIMS analysis. This prevents us from determining the mode of occurrence of these elements in the FGD-gypsums.

3.3. Potential leaching of FGD-gypsums at natural conditions

In addition to the potential mobility of Li, Ni, Cu, Zn, As, Se, Mo, and U from FGD-gypsums, the potential leaching of major elements such as Al, Ca, Fe, K, Mg, Mn, and Na has also been studied at the natural conditions (pH) of the FGD-gypsum leachates.

FGD-gypsum leachates are slightly alkaline with pH values ranging from 7.6 to 8.1 (Table 3). As a consequence, the leaching values of trace elements are relatively low. Arsenic is only detected in the FGD-G3 leachate. Sulphate and Ca show the highest leaching values in the FGD-gypsums because of gypsum dissolution.

The aqueous equilibrium calculations at 25°C and at the natural pH ($\text{pH} \sim 7$) of the FGD-gypsum leachates, reveals that AlO_2^- and $\text{Fe}^{2+}/\text{Fe}(\text{OH})_3$ are the predominant aqueous complexes of Al and Fe in the FGD-gypsum leachates (Table 2), whereas Na, K, Mg, Mn, Li, Cu, Ni, and Zn show the highest activities as free cations ($\text{X}^{n+1, 2}$) and as SO_4 -metal complexes (Table 3). The dissolution of gypsum and the relatively alkaline conditions of the FGD-gypsum leachates promote the formation and stability of SO_4 and OH-metal complexes in the FGD-gypsum leachates.

Molybdenum, As, Se, and U show the highest activities in the FGD-gypsum leachates as MoO_4^{2-} , HAsO_4^{2-} , HSeO_3^- , and $\text{UO}_2(\text{OH})_2$, respectively (Table 3). The stability of Mo, As, and Se aqueous complexes in the FGD-gypsum leachates can be associated to the relatively high mobility of oxy-anionic species and the slightly alkaline pH (7.4-7.6) of FGD-gypsum leachates. The stability of $\text{UO}_2(\text{OH})_2$ is attributed to its relatively high mobility under a wide pH (from 5.0 to 10.0) and Eh range (Eh>0, HCP, 2013).

3.4 Effect of pH

The role of the pH on the trace elements extraction was initially examined at a contact time of 24h, 25°C room temperature, and at 10:1 L/S ratio (Figure 1). The leaching results shown in this study are provided on average values.

The leaching values of most of the elements in the FGD-gypsum leachates increase when the pH decreases to 2.0. The increase of the leaching values of trace elements under the acidic conditions indicates that the FGD-gypsums undergo ion-exchange processes during leaching; elements are replaced by H^+ and dissolved into the aqueous phase from the gypsum particles.

3.4.1 Uranium

Uranium is the element with the highest leaching values in all the FGD-gypsums at the initial pH of 2.0 in comparison with the rest of the studied elements. The lowest leaching values of U occur at the natural pH of the FGD-gypsums (Figure 1). The sharp decrease of the U leaching as a function of the pH is significantly pronounced in the FGD-G2 and G4 leachates.

Although the ion-association aqueous modelling at the natural pH indicates $\text{UO}_2(\text{OH})_2$ as the predominant aqueous complex of U of the FGD-gypsum leachates, the FGD-G2 and G3 are slightly oversaturated with respect to $(\text{UO}_2)_2\text{SiO}_4 \cdot 2\text{H}_2\text{O}$, which potentially transfers U from leachates to solid phases (Table 2). By contrast, the FGD-gypsum leachates are undersaturated with respect to $(\text{UO}_2)_2\text{SiO}_4 \cdot 2\text{H}_2\text{O}$ and UO_2SO_4 and UO_2^{2+} are the aqueous complexes with the highest activities in the FGD-gypsum leachates at the initial pH of 2.0 (Table 3). The decrease of the $(\text{UO}_2)_2\text{SiO}_4 \cdot 2\text{H}_2\text{O}$ SI under acidic pHs indicates that the dissolution of

this specie potentially transfers U as $\text{UO}_2^{2+}(\text{aq})$ from the solid phase to the FGD-gypsum leachates.

According the thermodynamic model, it is postulated that $\text{UO}_2^{2+}(\text{aq})$ released from the $(\text{UO}_2)_2\text{SiO}_4 \cdot 2\text{H}_2\text{O}$ dissolution could immediately react with SO_4^{2-} (FGD-gypsum matrix) to form UO_2SO_4 aqueous complexes, and thereby increase the leaching of U as $\text{UO}_2\text{SO}_4(\text{aq})$ in the FGD-gypsum leachates.

3.4.2 Selenium

Selenium follows a similar pattern to that of U (Figure 1). The leaching values of Se are also the highest at the initial pH of 2.0 and the lowest at the natural pH in all the FGD-gypsum leachates. The ion-association aqueous modelling indicates that HSeO_3^- followed by $\text{SeO}_3^{2-}(\text{aq})$ are the predominant aqueous complexes of Se in the FGD-gypsum leachates at their natural pHs. By contrast, H_2Se presents the highest activity in the FGD-gypsum leachates at the initial pH of 2.0 (Table 4). The variation of the aqueous speciation of Se during leaching as a function of the pH indicates a reduction of Se species by the $\text{HSeO}_3^-(\text{aq}) + \text{H}^+ \leftrightarrow \text{H}_2\text{Se}(\text{aq})$ aqueous complexation reaction under the acidic conditions.

3.4.3 Nickel

Although Ni follows a similar behavior to that of U and Se, the pH variations during the FGD-gypsum leaching do not affect its aqueous speciation and stability in the leachates. For a Ni- H_2O system, Ni^{2+} is stable in acid and neutral solutions (HCP, 2013). This and the predominant $\text{SO}_4^{2-}(\text{aq})$ matrix of the FGD-gypsum leachates control the stability of Ni as a free cation (Ni^{2+}) as well as aqueous complex (NiSO_4) in the FGD-gypsum leachates (Table 4).

3.4.4 Zinc

Zinc reaches the highest leaching values in the FGD-G1 and G3 at the initial pH of 4.0 (Figure 1). In the FGD-G2 and G4, the leaching values of Zn are similar between 2.0 and 4.0 pHs but lower at the pH of 7.0. This leaching pattern suggests that the Zn-bearing species could be close to the equilibrium at which Zn reaches its maximum concentration in the FGD-gypsum

leachates at pH of 2.0 and 4.0. However, the undersaturation of FGD-gypsum leachates with respect to all Zn-bearing species at the initial pH of 2.0 and 4.0 prevent us from determining the behavior of Zn in the leachates in this pH range.

The variation of the SI for ferrite-Zn from the oversaturation at the natural pH of the FGD-gypsum leachates to the undersaturation at the pHs of 2.0 and 4.0, indicates that the mobility of Zn in the FGD-gypsum leachates could probably be controlled by the dissolution of this secondary mineral; since it could potentially transfer Zn from ferrite-Zn to the FGD-gypsum leachates.

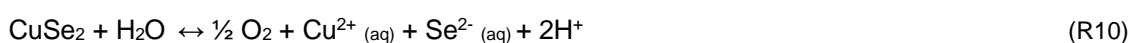
3.4.5 Lithium

Lithium reaches the highest leaching values in the FGD-gypsums at the initial pH of 2.0. The increase of the leaching values of Li when decreasing the pH can be attributed to the dissolution of Li_2SO_4 by ion-exchange processes during leaching; Li^+ and LiSO_4^- present the highest activities of Li in the FGD-gypsum leachates.

3.4.6 Copper

The leaching values of Cu are practically similar in the FGD-gypsum leachates at all the pHs (Figure 1). It is noticed a slight variation of the Cu leaching values in the FGD-G4 leachate, but this difference is not significant enough to be associated to the different pH values in the FGD-gypsum leachates. The oversaturation of the FGD-gypsum leachates with respect to CuSe_2 at an initial pH of 2.0, which would potentially transfers Cu^{2+} from the leachates to the solid phases, may explain the low leaching and mobility of Cu under acidic conditions.

Thus, it is postulated that in line with the FGD-gypsum leachate composition, the equilibrium of the above solid phase can be expressed as:



The thermodynamic reliability of the Cu_2Se precipitation can be demonstrated by comparing the actual Ionic Activity Product (IAP) obtained from the FGD-gypsum experimental data and the

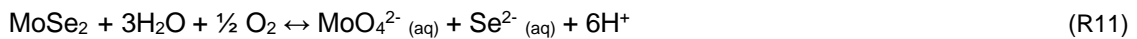
equilibrium constant (K) of the Cu₂Se formation derived from the thermodynamic database. The IAP is calculated as:

$$IAP = [aCu^{2+} \times aSe^{2-} \times a(H^+)^2] / [aCu_2Se \times aH_2O] \quad (R12)$$

where CuSe₂ is assumed to be the unity, aCu²⁺, aH⁺, and aSe²⁻ are calculated from their solute concentrations and the extended Debye-Huckel model (PHREEQc). The IAP calculated for the FGD-gypsum leachates is 10¹⁵ a long way above 10⁻¹¹⁶, which is the equilibrium constant of the Cu₂Se precipitation at 25°C. The IAP>K confirms the thermodynamic feasibility of the postulated process. Therefore, the relatively low leaching of Cu from FGD-gypsums at an initial pH of 2.0 might be associated to the precipitation of Cu₂Se under acidic conditions.

3.4.7 Molybdenum

The leaching values and speciation of Mo are also similar in the FGD-gypsum leachates at all the studied pHs (Figure 1). As for Cu, it is noticed a slight variation of the Mo leaching values in the FGD-G4 leachate, but it is not significant enough to be associated to the different pH values in the FGD-gypsum leachates. Despite the fact Mo is only mobile under alkaline conditions, the relatively low leaching and mobility of this element could be related with precipitation of a Mo-bearing species. According to the geochemical modelling, FGD-gypsum leachates are saturated with respect to MoSe₂ at the initial pH of 2.0. Thus, it is postulated that in line with the FGD-gypsum leachate composition, the equilibrium of the above solid phases can be expressed as:



As for Cu, the thermodynamic reliability of the MoSe₂ precipitation can be demonstrated by comparing the actual IAP obtained from the FGD-gypsum experimental data and the K of the MoSe₂ formation derived from the thermodynamic database. The IAP is calculated as:

$$IAP = [aMoO_4^{2-} \times aSe^{2-} \times a(H^+)^6] / [aMoSe_2 \times a(H_2O)] \quad (R12)$$

where MoSe_2 are assumed to be the unity, $a_{\text{MoO}_4^{2-}}$, a_{H^+} , and $a_{\text{Se}^{2-}}$ are calculated from their solute concentrations and the extended Debye-Huckel model (PHREEQc). The IAP calculated for the FGD-gypsum leachates is 10^{-43} a long way above 10^{-106} , which is the equilibrium constant of the MoSe_2 precipitation at 25°C . The $\text{IAP} > K$ confirms the thermodynamic feasibility of the postulated process. Therefore, the relatively low leaching of Mo from FGD-gypsums at an initial pH of 2.0 might be associated to the precipitation of MoSe_2 under acidic conditions.

3.4.8 Arsenic

Arsenic shows a different speciation in the FGD-gypsum leachates as a result of the different pH values. HAsO_4^{2-} shows the highest activity in the FGD-G3 at the natural pH of the FGD-gypsum leachate, whereas HAsO_2 is the aqueous complex with the highest activity in the FGD-G1 and G3 at the initial pH of 2.0 and 4.0. This ion-association aqueous modelling points out that the As species undergo a two-step reduction process as a consequence of the acidic conditions by the $\text{H}_2\text{AsO}_4^- + \text{H}^+ \leftrightarrow \text{HAsO}_2(\text{aq}) + \frac{1}{2} \text{O}_2 + \text{H}_2\text{O}$ aqueous complexation reaction.

From these results, it can be concluded that the pH has a significant influence in the potential leaching and speciation of elements because of its contribution to the precipitation and dissolution of minerals and solid phases. Most of the elements increase their potential leaching, and thereby their mobility, when decreasing the pH. By contrast, Cu and Mo tend to be transferred from the aqueous to solid phase of FGD-gypsums by the precipitation of CuSe_2 and MoSe_2 under acidic conditions. The $\text{IAP} < K$ of both precipitation reactions confirms the thermodynamic feasibility of the postulated processes.

3.5 Effect of solid-to-liquid (S/L) ratio

The effect of L/S ratio on the trace element extraction from FGD-gypsum samples was examined for 10:1, 20:1, and 50:1 L/S ratios, a contact time of 24h, at 25°C room temperature, and at the initial pH of 2.0 as a result of the maximum leaching of trace elements under these conditions.

It is found from Fig. 2 that the leaching rate for all the trace elements attains their maximum values at L/S ratio of 10:1 and no further drastic increase with increasing L/S ratios, except for Zn. Zinc reaches the equilibrium in the FGD-G1 and G3 leachates at the 50:1 L/S ratio. It is also noticed that the leaching rate for all the trace elements decreases significantly from the 10/1 to 20/1 L/S ratio, especially, in the FGD-G4 leachates. However, the leaching value of As and Cu in all the FGD-gypsum samples follow a different pattern. Arsenic is not detected in the FGD-G2 leachate in spite of the different L/S ratios, whereas Cu is only detected in the FGD-G2 at the 10:1 ratio. As and Cu are only detected in the FGD-G4 leachate at the 10:1 and 10:1 and 20/1 ratios, respectively.

3.6. Effect of contact time

In this article, the effect of the contact time on trace elements extraction from FGD-gypsums is only discussed for an initial pH of 2.0, 25°C room temperature, and at 10:1 L/S ratio as a result of the maximum leaching of trace elements under these conditions (Figure 3).

Lithium and U follow a similar leaching pattern in the FGD-gypsums along time; their leaching values increase from 24 to 48h and reach the equilibrium close to 168h. The leaching values of Mo and Ni reach the equilibrium close to 48h with the exception of the FGD-G4 leachate (Figure 3).

The leaching values of Cu and Zn tend to decrease from the 24 to 48h. However, their leaching values increase subsequent to 48h suggesting a transport-controlled release process. The leaching values of As decrease with time to levels below the limit of detection after 48h of leaching test. Arsenic reaches the equilibrium in the FGD-G2 close to 168h.

Selenium shows no consistent trend with time. In the FGD-G2 and G3, the leaching values of Se increase from 24 to 48h and reach the equilibrium subsequent to 168h, whereas in the FGD-G1 and G4, the leaching values of Se decrease showing no future equilibrium along leaching time.

From these results, it can be concluded that 24h is the acceptable time for effective extraction of trace elements from a solid by-product at its natural pH. However, it is important to highlight that acidic conditions tend to increase the potential leaching of some trace elements along time such as it has been demonstrated in this study.

4. CONCLUSIONS

Results show that the extraction rate of the studied elements generally increased with decreasing the pH value of the FGD-gypsum leachates, which suggests an environmental risk because of Li, Zn, Ni, As, Se, and U leaching. The reverse behaviour is found for Cu and Mo.

The increase of the mobility of U, Se, and As in the FGD-gypsum leachates as a result of the pH decrease entails the modification of their aqueous speciation in the leachates; UO_2SO_4 , H_2Se , and HAsO_2 are the aqueous complexes with the highest activities under acidic conditions. By contrast, the speciation of Zn, Li, and Ni is not affected in spite of pH changes; these elements occur as free cations and associated to SO_4^{2-} in the FGD-gypsum leachates. The mobility of Cu and Mo decreases by decreasing the pH of the FGD-gypsum leachates, which might be associated to the precipitation of CuSe_2 and MoSe_2 , respectively.

The leaching rate for all the trace elements attains their maximum values at L/S ratio of 10:1 and no further drastic increase with increasing L/S ratios, except for Zn. Zinc reaches the equilibrium at the L/S ratio of 50:1. Currently, 24h is the acceptable time for effective extraction of trace elements from a solid by-product at the natural pH of the corresponding solid by-product. However, it is important to highlight that acidic conditions tend to increase the potential leaching of some trace elements along time such as it has been demonstrated in this study.

Although minor solid phases of trace elements predicted thermodynamically in saturation were not identified by XRD, the identification of the structural components of such solid phases supports the precipitation processes of AlO_2H , AlHO_2 , $\text{KAl}_3(\text{OH})_6(\text{SO}_4)_2$, $\text{Al}(\text{OH})_3$, $\text{Al}_2\text{Si}_2\text{O}_5(\text{OH})_4$, $\text{KAl}_3\text{Si}_3\text{O}_{10}(\text{OH})_2$, CuFe_2O_4 , ZnFe_2O_4 , FeOOH , Fe_2O_3 , Fe_3O_4 in all the FGD-gypsum samples,

and $\text{Ca}_2\text{FeAl}_2\text{Si}_3\text{O}_{12}\text{OH}$, $\text{FeCa}_2\text{Al}_2(\text{OH})(\text{SiO}_4)_3$, $\text{CaAl}_2\text{Si}_2\text{O}_7(\text{OH})_2\cdot\text{H}_2\text{O}$, $\text{CaAl}_4\text{Si}_2\text{O}_{10}(\text{OH})_2$, and $\text{NaAl}_3\text{Si}_3\text{O}_{10}(\text{OH})_2$ in the FGD-G1 and FGD-G2 samples.

TOF mass spectrometry of the solid phase combined with thermodynamic modelling of the aqueous phase has proved useful in understanding the mobility and geochemical behaviour of elements and their partitioning into FGD-gypsum samples. Other techniques such as synchrotron light micro X-ray fluorescence, micro-XRD and X-ray absorption spectroscopies may constitute a more accurate approach to the identification of solid phases.

5. ACKNOWLEDGEMENTS

We would like to thank the staff of the Spanish power plants for their support, help, and kind assistance during and after the collection of the samples. The corresponding author gratefully acknowledges the Institute of Environmental Assessment and Water Research (IDAEA). Spanish Research Council (CSIC).

6. REFERENCES

- Córdoba, P., Font, O., Izquierdo, M., Querol, X., Tobías, A., López-Antón, M.A., Ochoa-González, R., Díaz-Somoano, M., Martínez-Tarazona, M.R., Ayora, C., Leiva, C., Fernández, C., Giménez, A. Enrichment of inorganic trace pollutants in re-circulated water streams from a wet limestone flue gas desulphurisation system in two coal power plants. *Fuel Process. Technol.* 2011; 92: 1764–1775.
- Córdoba P, Ayora C, Moreno N, Font O, Izquierdo M, Querol X. Influence of an aluminium additive in aqueous and solid speciation of elements in flue gas desulphurisation system *Energy* 50, (2013), 438-444.
- Sanchez F, Kosson D, Keeney R, Delapp R, Turner L, Kariher P. Characterization of coal combustion residues from electric utilities using wet scrubbers for multi-pollutant control. EPA/600/R-08/077, Washington DC, US Environmental Protection Agency; 2008
- Kairies, C. L.; Schroeder, K. T.; Cardone, C. R. Mercury in gypsum produced from flue gas desulfurization. *Fuel* 2006;85:2530–2536.

506 Kost, D. A.; Bigam, J. M.; Stehouwer, R. C.; Beeghly, J. H.; Fowler, R.; Traina, S. J.; Wolfe, W.
 507 E.; Dick, W. A. Chemical and physical properties of dry flue gas desulfurization products.
 508 J. Environ. Qual. 2005, 34 (2), 676–686.

509 Diaz-Somoano, M.; Martinez-Tarazona, M. R. Retention of arsenic and selenium compounds
 510 using limestone in a coal gasification flue gas. Environ. Sci. Technol. 2004;38: 899–903.

511 Guo, X.; Zheng, C. G.; Xu, M. H. Characterization of arsenic emissions from a coal-fired power
 512 plant. *Energy Fuels* 2004; 18:1822-1826.

513 Font, O., Querol, X., Moreno, T., Ballesteros, J.C., Giménez, A. Effect of aluminum sulphate
 514 addition on reducing the leachable potential of fluorine from FGD gypsum. In:
 515 proceedings of 2nd International Conference on Engineering for Waste Valorisation.
 516 Patras. Greece, ISBN: 978-960-530-101-9, 2008, p. 150.

517 EN-12457-4 Characterization of waste- Leaching-Compliance test for leaching of granular
 518 waste materials and sludges – Part 4: One stage batch test at a liquid to solid ratio of 10
 519 l/kg for materials with particle size below 10 mm (without or with size reduction).

520 Álvarez-Ayuso E, Querol X, Tomás A. Environmental impact of coal combustion-
 521 desulphurisation plant: Abatement capacity of desulphurisation process and
 522 environmental characterisation of combustion by-products. *Chemosphere* 2006; 665:
 523 2009-2017.

524 Álvarez- Ayuso, E., Querol, X. Stabilization of FGD gypsum for its disposal in landfills using
 525 amorphous aluminium oxide as fluoride retention. *Chemosphere* 2007; 69: 295–302.

526 Álvarez- Ayuso, E., Querol, X. Study of the use of coal fly ash as an additive to minimise
 527 fluoride leaching from FGD gypsum for its disposal. *Chemosphere* 2008; 71: 140–146.

528 Andrea Tabasová A., Kropáč J., Kermes V., Nemet A., Stehlík P. Waste-to-energy technologies:
 529 Impact on environment. *Energy* 2012; 44: 146-155.

530 Parkhurst, D.L., Appelo, C.A.J., 1999. User's guide to PHREEQC (version 2). A computer
 531 program for speciation, reaction-path, 1D-transport, and inverse geochemical
 532 calculations. US Geol. Surv. Water Resour. Inv. Rep. 99-4259, 312p.

533 Drever J.I. The geochemistry of natural waters: surface and groundwater environments. 3rd ed.
 534 New Jersey: Prentice Hall; 1997.

535 Jadhav, R. A.; Fan, L. S. Capture of Gas-Phase Arsenic Oxide by Lime: Kinetic and Mechanistic
536 Studies. *Environ. Sci. Technol.* 2001, 35 (4), 794–799.
537 Ghosh-Dastidar, A.; Mahuli, S.; Agnihotri, R.; Fan, L. S. Selenium Capture Using Sorbent
538 Powders: Mechanism of Sorption by Hydrated Lime. *Environ. Sci. Technol.* 1996, 30 (2),
539 447–452.
540 Handbook of Chemistry and Physics. 91 st ed. 2013-2014. Electronic version.
541

FIGURES

FIGURE 1. Leaching values of the selected elements vs. pH. 10/1 ratio and 24h contact time. a)FGD-G1, b) FGD-G2, c) FGD-G3, and d) FGD-G4.

FIGURE 2. Leaching values of the selected elements vs. L/S ratios. pH = 2.0 and 24h contact time. a)FGD-G1, b) FGD-G2, c) FGD-G3, and d) FGD-G4.

FIGURE 3. Leaching values of the selected elements vs. Contact time. pH = 2.0 and 10/1 ratio.

FIGURE 1

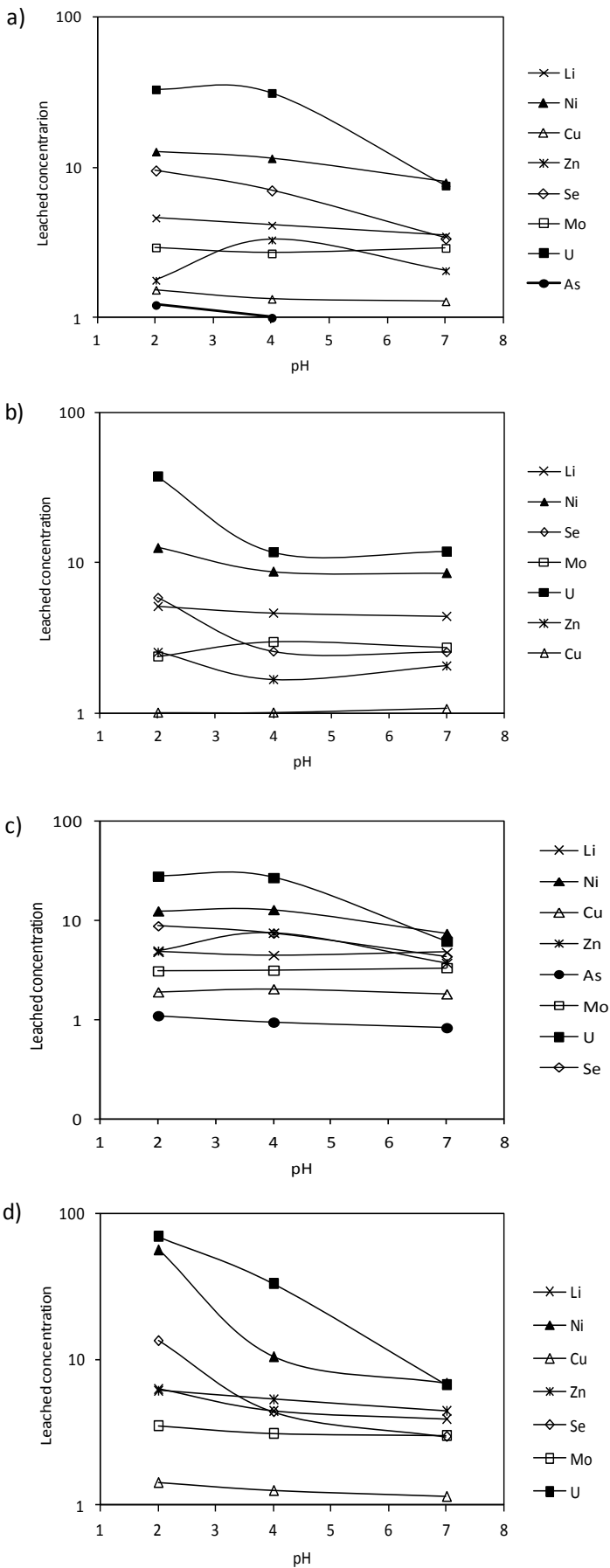


FIGURE 2

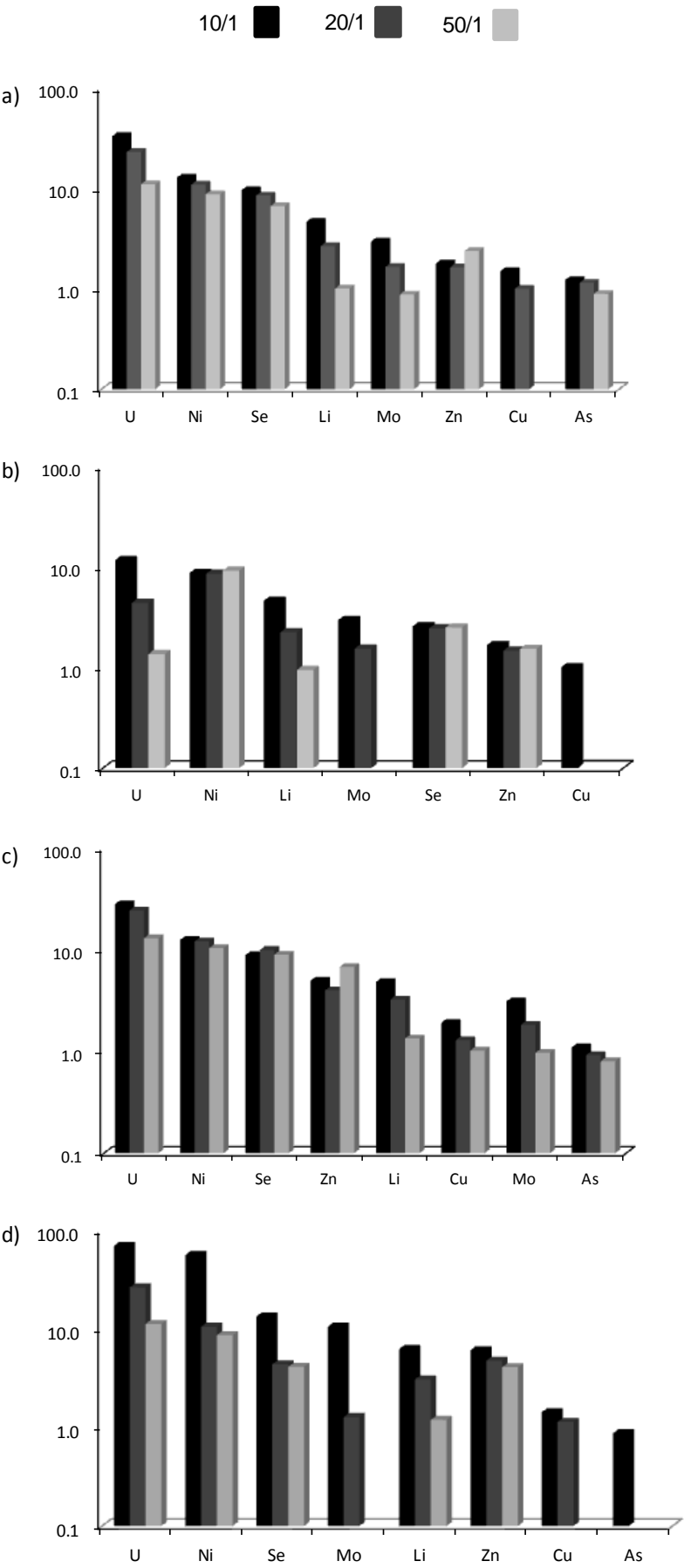
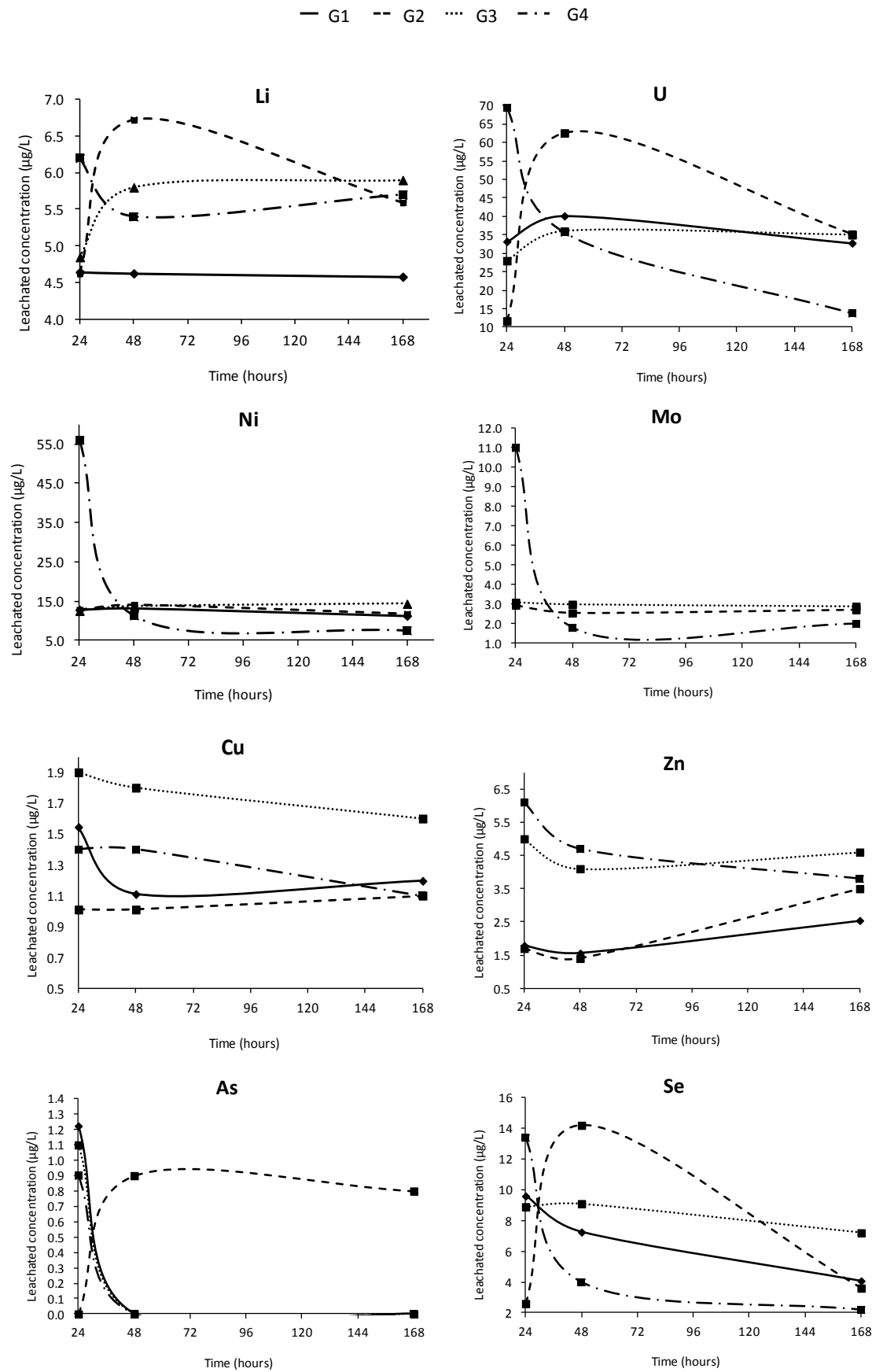


FIGURE 3



TABLES

TABLE 1. Intensity of the signal of molecules, clusters, and elements identified in FGD-gypsums

TABLE 2. Saturation indices of selected solid phases in FGD-gypsum leachates at their natural pH (~7).

TABLE 3. Leachable concentrations of selected elements in FGD-gypsum samples

TABLE 4. Aqueous speciation of trace elements in FGD-gypsum leachates at different pHs

TABLE 1

Molecules	Intensity (counts)			
	FGD-gypsum 1	FGD-gypsum 2	FGD-gypsum 3	FGD-gypsum 4
OH	288975	131100	78889	114573
SiO ₂	51921	45949	26359	31871
SO ₂	37517	40354	22950	10208
SiO ₃	54701	44747	21575	30664
SiHO ₃	46714	43318	21394	20445
SO ₃	24116	25378	16450	7412
SO ₄	9961	14807	7292	3669
HSO ₄	7872	12439	3976	2338
Se ₂ O ₃	738	1441	1074	696
CaOH	10269	23952	15879	9522
Ca ₂ O ₂	3333	7186	5561	3300
Al	13308	16007	24320	10105
Li	1505	1768	1679	704
Na	29490	49300	34261	20108
Mg	15522	22550	19764	11140
K	75932	80786	127743	64865
Ca	15306	25128	28576	17191
Fe	1999	2539	3387	1627
Mn	336	253	607	189
As	99	172	167	92
Se	769	1237	665	445
Zn	239	403	281	144

TABLE 2

SATURATION INDEX (log IAP/Ksp)					
	SOLID PHASES	FGD-G1	FGD-G2	FGD-G3	FGD-G4
Al	AlO ₂ H	2.72	2.72	2.97	2.72
	AlHO ₂	3.13	3.09	3.37	3.13
	KAl ₃ (OH) ₆ (SO ₄) ₂	1.29	1.35	2.10	1.29
	Al(OH) ₃	3.13	2.53	2.78	2.53
	Al ₂ Si ₂ O ₅ (OH) ₄	3.22	3.67	4.16	3.47
	KAl ₃ Si ₃ O ₁₀ (OH) ₂	-	4.76	5.50	4.39
Ca	Ca ₂ FeAl ₂ Si ₃ O ₁₂ OH	-0.26	-0.90	1.56	-0.63
	FeCa ₂ Al ₂ (OH)(SiO ₄) ₃	-0.27	-0.91	1.57	-0.64
	CaAl ₂ Si ₂ O ₇ (OH) ₂ ·H ₂ O	-0.43	0.0	0.49	-0.18
	CaAl ₄ Si ₂ O ₁₀ (OH) ₂	-1.29	-1.72	2.71	-1.54
	NaAl ₃ Si ₃ O ₁₀ (OH) ₂	-0.56	-1.23	2.05	-0.94
Fe	CuFe ₂ O ₄	5.17	5.18	5.83	5.17
	ZnFe ₂ O ₄	4.13	4.14	4.79	4.13
	FeOOH	4.39	4.40	4.57	4.39
	Fe ₂ O ₃	9.77	9.78	10.13	9.77
	Fe ₃ O ₄	6.37	6.38	6.91	6.37
U	(UO ₂) ₂ SiO ₄ ·2H ₂ O	-	0.35	0.38	0.06

TABLE 3

	FGD-G1	FGD-G2	FGD-G3	FGD-G4
pH	7.8	7.5	7.1	8.1
mg/L				
Al	0.1	0.1	0.2	0.1
Ca	609	587	584	564
Fe	0.02	0.02	0.03	0.02
K	1.8	2.1	2.1	1.8
Mg	34	34	41	37
Na	3.1	3.1	3.7	4.1
SO ₄ ²⁻	1585	1543	1564	1459
µg/L				
Li	3.5	4.4	4.8	3.9
Mn	402	342	535	286
Ni	8.0	8.5	7.4	6.8
Cu	1.3	1.1	1.8	1.1
Zn	2.1	2.1	3.8	4.4
As	<0.01	<0.01	0.8	<0.01
Se	3.4	2.5	4.4	3.0
Rb	0.8	0.9	1.0	1.0
Mo	2.9	2.7	3.4	1.5
U	7.6	12	6.2	6.7

TABLE 4

		FGD-G1	FGD-G2	FGD-G3	FGD-G4
Li	pH2	$\text{Li}^+/\text{LiSO}_4^-$	$\text{Li}^+/\text{LiSO}_4^-$	$\text{Li}^+/\text{LiSO}_4^-$	$\text{Li}^+/\text{LiSO}_4^-$
	pH4				
Ni	pH2	$\text{Ni}^{2+}/\text{NiSO}_4$	$\text{Ni}^{2+}/\text{NiSO}_4$	$\text{Ni}^{2+}/\text{NiSO}_4$	$\text{Ni}^{2+}/\text{NiSO}_4$
	pH4				
Cu	pH2	$\text{Cu}^{2+}/\text{CuSO}_4$	$\text{Cu}^{2+}/\text{CuSO}_4$	$\text{Cu}^{2+}/\text{CuSO}_4$	$\text{Cu}^{2+}/\text{CuSO}_4$
	pH4				
Zn	pH2	Zn^{2+} ZnSO_4	Zn^{2+} ZnSO_4	Zn^{2+} ZnSO_4	Zn^{2+} ZnSO_4
	pH4				
As	pH2	HAsO_2	-	HAsO_2	-
	pH4				
Se	pH2	H_2Se HSeO_3^-	H_2Se HSeO_3^-	H_2Se HSeO_3^-	H_2Se HSeO_3^-
	pH4				
Mo	pH2	MoO_4^-	MoO_4^-	MoO_4^-	MoO_4^-
	pH4				
U	pH2	$\text{UO}_2^{2+}/\text{UO}_2\text{SO}_4$	$\text{UO}_2^{2+}/\text{UO}_2\text{SO}_4$	$\text{UO}_2^{2+}/\text{UO}_2\text{SO}_4$	$\text{UO}_2^{2+}/\text{UO}_2\text{SO}_4$
	pH4				